WPPFC-CPR(17) 17093

S Brezinsek et al.

Spectroscopic determination of inverse photon efficiencies of W atoms in the scrape-off layer of TEXTOR

Preprint of Paper to be submitted for publication in Proceeding of 16th International Conference on Plasma-Facing Materials and Components for Fusion Applications

This work has been carried out within the framework of the EUROfusion Consortium and has received funding from the Euratom research and training programme 2014-2018 under grant agreement No 633053. The views and opinions expressed herein do not necessarily reflect those of the European Commission.

This document is intended for publication in the open literature. It is made available on the clear understanding that it may not be further circulated and extracts or references may not be published prior to publication of the original when applicable, or without the consent of the Publications Officer, EUROfusion Programme Management Unit, Culham Science Centre, Abingdon, Oxon, OX14 3DB, UK or e-mail Publications.Officer@euro-fusion.org

Enquiries about Copyright and reproduction should be addressed to the Publications Officer, EUROfusion Programme Management Unit, Culham Science Centre, Abingdon, Oxon, OX14 3DB, UK or e-mail Publications.Officer@euro-fusion.org

The contents of this preprint and all other EUROfusion Preprints, Reports and Conference Papers are available to view online free at http://www.euro-fusionscipub.org. This site has full search facilities and e-mail alert options. In the JET specific papers the diagrams contained within the PDFs on this site are hyperlinked

Spectroscopic Determination of Inverse Photon Efficiencies of W Atoms in the Scrape-Off Layer of TEXTOR

S. Brezinsek[◇], M. Laengner, J.W. Coenen, A. Pospieszczyk

G. Sergienko, U. Samm

Forschungszentrum Jülich GmbH, Institut für Energie- und Klimaforschung - Plasmaphysik, 52425 Jülich, Germany

Abstract

Optical emission spectroscopy can be applied to determine in-situ tungsten particle fluxes from erosion processes at plasma-facing materials. Inverse photon efficiencies convert photon fluxes of WI and WII line transitions into W and W^+ particle fluxes, respectively, in dependence on the local plasma conditions. Experiments in TEXTOR were carried out to determine effective conversion factors for different WI and WII transitions with the aid of WF_6 injection into the deuterium scrape-off layer plasmas in the electron temperature range between $T_e = 20eV$ and $T_e = 82eV$. The inverse photon efficiencies or so-called effective $\frac{S}{XB}$-values have been determined for WI lines at $\lambda = 400.9nm$, $429.5nm$, $488.7nm$, and $522.5nm$ as well as WII at $\lambda = 434.6nm$ and compared with theoretical calculations from the ADAS data base. Moreover, a multi-machine scaling for the $\frac{S}{XB}$-value between $T_e = 2...100eV$ has been determined for the most prominent WI line at $\lambda = 400.9nm$ to $\frac{S}{XB}(T_e) = 53.63 - 56.07 \times e^{(0.045 \times T_e[eV])}$ considering experimental data from TEXTOR, ASDEX Upgrade, PSI, and PISCES. Comparison with ADAS calculations for the same transition reveal a good general dependence on the general dependence on T_e, but the an overestimation of about 50% in the theoretical calculations over the full covered range of T_e. The same overestimation of theoretically calculated $\frac{S}{XB}$-values from ADAS has been observed for WI at $\lambda = 429.5nm$ and $\lambda = 522.5nm$ indicating potentially to an overestimation of applied ionisation rate coefficients in ADAS for neutral W.

[◇]*Corresponding author address:* Forschungszentrum Jülich GmbH, Institut für Energie und

Klimaforschung Plasmaphysik, 52425 Jülich, Germany

◇*Corresponding author telephone:* +49 2461 616611

◇*Corresponding author e-mail:* s.brezinsek@fz-juelich.de

1 Introduction

Tungsten (W) is foreseen as material for the divertor plasma-facing components (PFCs) in the next fusion device ITER [1] and has been extensively used in recent years in the ASDEX-Upgrade [2] and the JET tokamak equipped with the ITER-like Wall material configuration [3]. Apart from the severe challenging issue of power handling compatibility of W-based PFCs with the plasma exhaust, in particular under the impact of fast transients like Edge Localised Modes (ELMs) [4], the most important issue concerning the use of W PFCs is the W source strength and its control. The W source is on the one hand via erosion processes directly related to the lifetime of divertor PFCs, and on the other hand, via W transport processes related to the concentration of W in the plasma core. The latter potentially can inhibit in a reactor the fusion process if a critical W concentration in the core of $O(10^{-5})$ has been exceeded [5]. Therefore, quantification of the W source or the W influx to the plasma is most important for the sustainable application of W in future fusion devices.

W erosion in steady-state conditions is dominated by impinging intrinsic impurities such as Be, O, C or extrinsic species like N or Ne, but not by impinging hydrogenic fuel species as previous studies in TEXTOR [6], ASEDX Upgrade [7], and JET in quiet L-mode conditions have shown [8]. Recent JET-ILW studies confirmed the importance of ELM-induced W sources in H-mode plasmas as previously reported in ASDEX Upgrade [7], but revealed n addition that at ion impact energies above $E_{in} = 1keV$, as present during an ELM impact

in JET, hydrogenic species ($H,\ D$) cause and even dominate the W sputtering process in the divertor [9]. Access to the W source strength and the associated W impurity influx during plasma operation is given in-situ solely by optical emission spectroscopy of neutral and singly ionised W of which the corresponding emission lines are preferable in the ultraviolet and blue spectral region [10]. Thus, the determination of the W sputtering flux is based on the application of (empirical) inverse photon efficiencies, so-called $\frac{S}{XB}$-values, on neutral W line emission, in particular at the most prominent WI transition at $\lambda = 400.9nm$ as previously reported [6] where for the first time WF_6 injection has been applied for in-situ W influx calibration.

Here, we present results from a series of experiments with local WF_6 injection into the plasma edge layer of TEXTOR providing effective inverse photon efficiencies for a set of prominent WI lines in the visible range in addition to the standard line at $400.9nm$. In comparison to the proof-of-principle experiment reported before [6], not only more WI lines were studied, but also a wider range of plasma conditions covered: electron temperatures T_e between $20eV$ and $85eV$ and electron densities n_e between $2.0 \times 10^{18}m^{-3}$ and $1.0 \times 10^{19}m^{-3}$. The earlier experiment has been also carefully revisited and additional spectroscopic systems in the analysis included providing effective photon efficiencies for WI lines at $429.5nm$, $488.7nm$, $498.3nm$, $505.3nm$, and $522.5nm$ [11]. The experimentally determined effective $\frac{S}{XB}$-values were compared with recent calculations provided by the ADAS database [12]. Moreover, a multi-machine scaling within International Tokamak Physics Agreement for the $\frac{S}{XB}$-value of the standard WI line at $\lambda = 400.9nm$ has been derived and compared with ADAS, considering experimental values at the lower T_e-range from three additional fusion-relevant experiments: PSI [15], PISCES [13], and ASDEX Upgrade [14].

2 Experiment

The experimental se-up is comparable to the one described in [6] with the gas inlet tube positioned in the near Scrape-Off Layer (SOL) of TEXTOR within $1cm$ to $4cm$ distance from the Last-Closed-Flux Surface (LCFS) in the lower limiter lock system. The injection cloud was observed spectroscopically by multiple interference filtered cameras in the visible range and set of spectrometer systems [16] which complement each other and provide the required spatial, temporal, and spectral information to analyse the multiple WI and WII line emission out of the injection and dissociation of WF_6 in W and ionisation into W^+, respectively. Cross sections of the line-of-side chords at the gas inlet location are depicted in fig. 1a). Accordingly, fig. 1b) shows a typical emission cloud of the standard WI transition $5d^5(^6S)6s\ ^7S_3 \rightarrow 5d^5(^6S)6p\ ^7P_4$ at $\lambda = 400.9nm$ recorded with an image intensified 2D camera equipped a narrowband interference filter (FWHM: $1.0nm$ at $\lambda = 400.9nm$) in front of the gas inlet tube which has been mostly studied in this contribution. Temporal information of the injection process in the plasma was obtained by a compact spectrometer system in Czerny-Turner arrangement (Avaspec, wavelength span: $195 - 463nm$, spectral resolution: $0.13nm/pix$, FWHM: $3pix$, exposure time: $32m$) observing the integral emission of the standard WI line whereas the detailed line analysis of additional transitions was done with the aid of a cross-dispersion spectrometer (Spectrelle) with an almost constant resolving power of more than $R = \frac{\lambda}{\Delta\lambda} \geq 20000$ over the full covered spectral range of $364 - 715nm$. The price for the simultaneously obtained high resolution spectrum with wide wavelength span is the relative low sensitivity of the system [17] and the lower temporal resolution of typically $200ms$ used in these measurements. Comparison with the 2D camera impages, described in more detail in [6, 17], ensured that the observation chords are aligned in a way that the full detection of WI or WII emission is guaranteed. However, both systems deviate

systematically about 25% in the radiometric calibration which could not be resolved, but this difference is still within the experimental uncertainties of the photon flux determination obtained by the individual systems [17]. The majority of analysis is done with the Spectrelle system which shows systematically a slightly higher inverse photon efficiency in comparison with the compact spectrometer estimates; the difference is indicated by notation to corresponding values as well as in the multi-machine scaling in the next section 3 for both systems based on the same experiment.

WF_6 is promptly dissociated at the given high temperature conditions present in the TEXTOR plasma edge of more than $T_e = 20eV$ as $T_e \gg T_{diss}^{WF_6}$ with $T_{diss}^{WF_6} = (600 - 1100)K$ is always fulfilled [18]. Though a low $T_{diss}^{WF_6}$ is useful to mimic effectively an atomic W injection beam entering the edge plasma, it is associated with the risk that WF_6 is dissociated within the metallic gas inlet tube and a fraction of produced W atoms is immediately deposited on the tube wall instead of penetrating the plasma. In order to study this effect, a dedicated experiment (***expA***) with electrically pre-heatable gas inlet was carried out [17]. A series of identical deuterium plasmas in standard TEXTOR conditions for these type of plasma-wall interaction studies ($I_p = 0.35MA, B_t = 2.25T, P_{aux} = 1.3MW$) were executed with increasing gas inlet temperature T_{inlet} from discharge to discharge by electrical pre-heating, but keeping the effective injection rate of WF_6 (Γ_{WF_6}) and the radial position of the gas inlet (r_{inlet}) constant in all discharges at $\Gamma_{WF_6} = 1 \times 10^{19} s^{-1}$ and $r_{inlet} = r_{LCFS} - 2cm$. Only pulsed injections were possible because of the applied gas injection system in the limiter lock with low conductance due to the thin and $2m$ long connection tube between gas reservoir and the gas inlet as well as the restricted flat-top phase of the plasma discharge of t$3s$ to $5s$ duration. In fig. 1c) and the curve indicated with $T_{inlet} = 494K$ is the typical time evolution of the standard WI emission with respect to the plasma flat-top phase indicated. The temporal evolution of WI emission has always been simulated by a pulse function in order

to quantify the total amount of photons, considering the loss fraction of photons related to the premature end of the flat-top phase and compared with the amount of injected WF_6 deduced from the pressure drop in the gas reservoir filled with WF_6. Additionally, fig. 1c) visualises the impact of the WF_6 dissociation process within the electrically pre-heated tube and subsequent local W deposition on the tube walls on the WI emission in the plasma as function of T_{inlet} between $499K$ and $1094K$. Clearly a decrease of the WI emission can be observed when $T_{inlet} = 723K \geq T_{diss}^{WF_6}$ was reached and collisions of the molecules with the tube wall provided the required energy for molecular dissociation and local deposition of the so dissociated W on the tube walls occurred. The drop in WI emission continues with higher T_{inlet} up to the maximum externally applied temperature of $T_{inlet} = 1094K$ where most of the injected gas remained in the gas inlet tube as W deposit. Repetition of a discharge after a long cool down phase at the end of the experimental day with $T_{inlet} = 766K$ showed a slight lower WI photon flux in comparison with a measurement in the heat-up phase; the difference may be attributed to the significant local W deposition within the metallic gas inlet tube which has been confirmed by destructive post-mortem analysis. For the experiments related to the quantification of the inverse photon efficiencies discussed in the next section 3, T_{inlet} was ensured to be below the experimental dissociation temperature onset $T_{diss}^{WF_6} \simeq 600K$ of WF_6 and controlled by thermocouple measurements in the standard type of gas inlets without active electrical pre-heating. For completeness it shall be mentioned that for a subset of experiments presented here also penetration depths of WI have been recorded and analysed by a Czerny-Turner spectrometer with radial resolution [19], effective velocities of the injected WF_6 and W atoms modelled [20], and ionisation rates experimentally determined and compared with theoretical calculations (ADAS, GKU, and Lotz) [17]. The corresponding analysis is outside of the scope of this paper, but it shall be stressed that the experimental ionisation rates tend to be systematically lower than the theoretical once

from the different calculations.

Though plasma conditions at the location of the gas injection were not accessible in the experiments presented here, the plasma edge profiles $n_e(r)$ and $T_e(r)$ between $r = r_{LCFS} - 1.0cm$ in the confined region and $r = r_{LCFS} + 3.5cm$ in the SOL were recorded with aid of one of the Helium beam diagnostics installed in TEXTOR and routinely used for edge characterisation [21, 22]. The single pair of T_e and n_e values applied in the next section (3) refer to these diagnostics and the plasma conditions at the maximum of WI light emission. The global discharge conditions remained equal to the TEXTOR standard ones mentioned before ($I_p = 0.35MA, B_t = 2.25T, P_{aux} = 1.3MW$), but with changes in the global deuterium puffing rate in order to vary T_e between $20eV$ and $85eV$ as well as simultaneously n_e between $1.0 \times 10^{19}m^{-3}$ and $2.0 \times 10^{18}m^{-3}$ for parametric scans (***expB***). We refer to [23] for detailed information about the transferability of the edge plasma parameters at different toroidal and poloidal locations to the location of the gas inlet in the lower limiter lock system.

In order to assess if a local perturbation is caused by the injected WF_6, in a supportive experiment (***expC***) the linearity between the standard WI photon flux at $400.9nm$ and the effective injected W particle flux, varied by the WF_6 injection rate, has been verified in the injection range between $\Gamma_{WF_6} = 7.5 \times 10^{18}s^{-1}$ and $\Gamma_{WF_6} = 2.0 \times 10^{19}s^{-1}$. The standard conditions described in (***expA***) were used and the standard gas inlet tube positioned at $r_{inlet} = r_{LCFS} - 2cm$. The radial position of the WI emission peak remained spatially constant below an injection rate of $1.25 \times 10^{19}s^{-1}$ whereas at values above a movement of WI emission peak towards the plasma can be observed which indicates moderate perturbation of the edge plasmas by local cooling caused by both the dissociation process itself as well as radiation of break-up products W and F out of WF_6 [17]. Therefore, in the two main experiments discussed in section (3), ***expB*** with plasma condition variation and fixed inlet position at $r_{inlet} = r_{LCFS} + 2.5cm$ and ***expD*** with constant edge plasma conditions and var-

ied inlet position between $r_{inlet} = r_{LCFS} + 4.0cm$ and $r_{inlet} = r_{LCFS} + 2cm$, all WF_6 injection rates were ensured to be below $\Gamma_{WF_6} < 1.0 \times 10^{19} s^{-1}$ and the gas inlet temperature below $T_{inlet} < 600K$ to permit as much as possible perturbation-free determination of effective inverse photon efficiencies for different WI transitions.

3 Experimental determination of effective inverse photon efficiencies for WI and WII in TEXTOR

The plasma edge layer in the limiter tokamak TEXTOR gives access to hot plasma conditions in the scrape-off layer in the range of T_e between $20eV$ and $85eV$ which reflects ionising conditions. This ionising plasma is therefore the valid regime for the usage of so-called $\frac{S}{XB}$-values (with S for ioniSation, B for Branching ratio, and X for excitation) or inverse photon efficiencies for conversion of spectroscopic photon fluxes into particle fluxes, or, in the present case to experimentally determine these conversion factors by comparing the injected particle flux with the associated photon flux. As the plasma conditions in the SOL are not constant, but have gradients, the usage of $\frac{S}{XB}$-values is simplification, however, the location where the ionisation and excitation takes places is spatially restricted, thus, the simplification is justified [24]. In this study, the focus is on conversion factors of in particular W atoms entering the edge plasma by erosion processes and optically emitting photons after electron impact excitation. However, as no pure gaseous W atomic source is available, WF_6 has been used as pre-courser assuming that the dissociation of the molecule in the plasma takes place almost instantly as discussed above in section 2. However, as the dissociation is included in the source term, we will in the next paragraph refer to effective inverse photon efficiencies or $S/XB_{WI}^{WF_6 \rightarrow W}$-values with WI denoting to the particular spectroscopic transition of neutral

W. Nevertheless, we assume that the experimental and calculated $\frac{S}{XB}$-values from ADAS can directly be compared considering the previous caveats and experimental conditions concerning injected WF_6 fluxes and gas inlet temperatures.

The two experiments **expB**, a series with varying plasma conditions by global deuterium fuelling and constant gas inlet position, and **expD**, a series of constant plasma conditions and varying radial position of the gas inlet in the SOL, were used to provide a data base for the dependence studies of $S/XB^{WF_6\rightarrow W}_{WI\ 400.9nm}$ on the plasma parameters T_e and n_e depicted in fig. 2. Both plasma parameters were varied at the same time, thus, the parameters are obtained pairwise. $S/XB^{WF_6\rightarrow W}_{WI\ 400.9nm}$ drops slightly with increasing edge density as shown in fig. 2a). Note that the values deduced in **expD** are systematically slightly lower, which may indicate indeed a minor perturbance in the radial scan experiment as the constant injected WF_6 flux is entering a region with lower plasma pressure in the SOL, thus, the measures values might correspond to a colder local plasma. We therefore exclude for the other WI transitions the data from **expD** series and focus on plasma from series **expB**. The more important parameter for the electron impact ionisation and excitation is the electron temperature and fig. 2b) shows the corresponding dependence of $S/XB^{WF_6\rightarrow W}_{WI\ 400.9nm}$ on T_e. There is a slight increase of the conversion factor with rising T_e, but obviously is the TEXTOR inverse photon efficiency data already at the high T_e range where the rate coefficients for ionisation and excitation are almost constant resulting in a constant effective $\frac{S}{XB}$. It would be justified on basis of this data to define a constant, averaged $S/XB^{WF_6\rightarrow W}_{WI\ 400.9nm} = 50$ (Avapsec) for the standard WI line which would be within the error bars of each individual measurement. The constant value is also applicable to WI photons caused by atoms which result from ELM-induced W sputtering which occurs at such high or even higher local T_e values.

The experimental data for the WI transition $5d^5(^6S)6s\ ^7S_3 \rightarrow 5d^5(^6S)6p\ ^7P_2$ at $\lambda = 429.5nm$, the WI transition $5d^4(^5D)6s^2\ ^5SD_4 \rightarrow 5d^4(^5D)6s6p\ ^7F_5$ at $\lambda = 488.7nm$, and

WI transition $5d^46s^2\ ^5D_3 \rightarrow 5d^46s(^6D)6p\ ^7D_2$ at $\lambda = 522.5nm$ can be analysed in the same manner as for the standard WI transition at $\lambda = 400.9nm$. The different $S/XB_{WI}^{WF_6 \rightarrow W}$ show all the same type of weak dependence on T_e and n_e in the covered plasma parameter range as it can be seen in fig. 3a). Thus, the same justifiable approach of a constant, averaged effective S/XB-value is possible, leading to the following set of values: $S/XB_{WI\ 429.5nm}^{WF_6 \rightarrow W} = 77$ (Avaspec), $S/XB_{WI\ 488.7nm}^{WF_6 \rightarrow W} = 347$ (Spectrelle), and $S/XB_{WI\ 522.5nm}^{WF_6 \rightarrow W} = 441$ (Spectrelle) in the range of $T_e = 20....85eV$. The correct identification of the mentioned set of WI lines can deduced from fig.3b where the measured and modelled line shapes on basis of a Zeeman-splitting analysis are visualised for the given toroidal magnetic field of $B_t = 2.25T$ in the TEXTOR experiment. There is a good agreement between modelled and measured WI line shapes for all lines studied in the WF_6 injection experiments. Moreover, fig.3a) shows the corresponding S/XB-values taken from ADAS as function of T_e for a typical span of n_e present in fusion plasmas. Clearly, it can be concluded that the TEXTOR data falls in the flat part of the $S/XB(T_e)$ curves as discussed before. S/XB-values for WI at $\lambda = 400.9nm$, $\lambda = 429.5nm$, and $\lambda = 522.5nm$ are in a fair agreement with the ADAS calculations, though for the three presented cases the experimental values are clearly lower than the calculated ones. The only very strong deviation of more than one order in magnitude can be found for the neutral W line transition at $\lambda = 488.7nm$ where the experimental values are in addition also higher than the calculated ones. This might indicate that the corresponding ADAS calculations are wrongly attributed to the assigned WI transition.

Fig. 4 addresses the effective inverse photon efficiency for a clearly identified WII transition which is suitable to determine the particle flux of singly charged W ions in the plasma edge. In fig.4a) is $S/XB_{WII\ 434.8nm}^{WF_6 \rightarrow W^+}$ in the standard T_e range of experiment **expB** depicted. In contrast to the corresponding plots for the WI transitions, a clear increase of the effective inverse photon efficiency is observable with increasing T_e. Fig. 4b) shows the correspond-

ing line shape analysis with Zeeman-splitting simulation for the applied magnetic field of $B_t = 2.25T$. The shape is well reproduced, however, it is important to state that this WII lines is challenging to observe in the W sputtering experiments at the same magnetic field strength. This is caused by the fact that in W erosion experiments, prompt re-deposition of W plays an important role, thus, a significant fraction of the eroded W is ionised, but not capable to radiate WII photons owing to immediate deposition on the W surface within the first Larmor radius. Secondly, the WII line is close to an OII transition and can be blended if the oxygen impurity content in the plasma is in the percentage range. Therefore, modelling of the line shape and background subtraction is required in W sputtering experiments employing this WII transition which is close to WI at $\lambda = 429.5nm$ and allow usually simultaneous detection and assessment of prompt re-deposition factors.

The TEXTOR data for $S/XB^{WF_6 \rightarrow W}_{WI\ 400.9nm}$ is most suitable to verify the corresponding ADAS calculations in the high electron temperature range with $T_e \geq 20eV$, but is not applicable to extrapolate to the low electron temperature range with $T_e < 20eV$. To validate the ADAS calculations in the complete fusion edge relevant temperature range, a multi-machine analysis was performed combining effective $\frac{S}{XB}$-values from TEXTOR and complementary $\frac{S}{XB}$ data sets in the range of $T_e < 20eV$ obtained from linear plasma devices PSI [15] and PISCES [13], determined via mass loss and optical emission spectroscopy, and from the ASDEX Upgrade divertor [14], determined via $W(CO)_6$ evaporation and optical emission spectroscopy. In fig. 5 is the full set of data up to a electron temperature of $100eV$ displayed with a region of overlap between all experiments at about $T_e = 20eV$. The TEXTOR set of data obtained from the compact spectrometer (Avaspec) fits best to the other experiments in the overlap region and used for the subsequent comparison. A least-square root fit routine was applied to the multi-machine data set including the individual error bars, resulting in a T_e-dependent fit function for the standard WI transition at $\lambda = 400.9nm$:

$\frac{S}{XB}(T_e) = 53.63 - 56.07 \times e^{(0.045 \times T_e[eV])}$ which is indicated in fig. 5 together with corresponding ADAS claculations. The shape of the experimental and calculated $S/XB^{W}_{WI\ 400.9nm}(T_e)$ is similar over the complete covered temperature range, but the ADAS data is systematically about 50% over the multi-machine fit based on experimental data. A potential cause could be an overestimation of the applied ionisation rates for neutral W in ADAS as suggested by the accompanied W penetration depths studies mentioned before. Moreover, it is supported by the fact that the effective S/XB-values for the tree WI lines at $\lambda = 400.9nm$, $\lambda = 429.5nm$, and $\lambda = 522.5nm$ in TEXTOR showed a similar deviation with ADAS calculations which overestimate experimental values in the range of $T_e = 20eV$ and $T_e = 85eV$.

4 Summary and Conclusion

The ability to determine in-situ the W erosion flux from plasma-facing components in fusion devices plays a key role with respect to life time estimates of PFCs as well as to the W source control in the next step fusion device. Optical emission spectroscopy observing the sputtered W atoms from the interacting W surface is one of the few available diagnostics which provides in-situ access to the W erosion flux as well as the capability to be used for W source control. Interpretation of the spectroscopic signals is done with the aid of inverse photon efficiencies which permit the conversion of photon fluxes of WI to particle fluxes of eroded W whereas the excitation of the released neutral W is done by electron impact excitation from the complex ground state population of the W atom. It should be stressed that spectroscopy of neutral WI alone provides access to the gross erosion, thus, not considering in the first place prompt re-deposition. The net erosion can be estimated if the prompt re-deposition factor is known which can be e.g. deduced from the escaping W ion if the emitting WII light is measured simultaneously. In this work, the required conversion factors for

the interpretation of different WI lines and one WII line were determined experimentally via the injection of WF_6 gas into the SOL of TEXTOR deuterium plasmas. By absolute calibration of the amount of injected molecules and under consideration of a low gas inlet temperature, which avoids pre-dissociation and local deposition in the inlet, as well as the radiometric calibration of the spectroscopic detection systems, providing photon fluxes of diverse WI lines, a set of empirical, or better, effective S/XB-values in the accessible high temperature plasma parameter range of TEXTOR were obtained. The major uncertainty in the experiment is not in the prompt dissociation of WF_6 or local perturbance of local plasma conditions by radiative cooling effects caused by W and F ionisation, but rather in the radiometric calibration of the different spectroscopic systems. The latter lead to unresolved discrepancies of about 25% for the two applied independent spectrometer systems with integral view on the emission cloud of WI, though the determined effective S/XB-values for the most prominent WI line at $\lambda = 400.9nm$ are still within the uncertainties of the two systems.

The focus of the presented studies was set to the determination of effective inverse photon efficiencies for WI and WII as well as more detailed study of the T_e and n_e dependence of the standard WI line. The effective S/XB-values at the high T_e range obtained in TEXTOR complement experimental values at the low T_e range obtained predominantly in linear plasma devices with an overlap region around $T_e = 20eV$. The available set of data from the different devices was combined to obtain a multi-machine fit for a value of $S/XB^{W}_{WI\ at\ 400.9nm}$ in the experimentally covered range of $T_e = 2eV$ and $T_e = 82eV$. This multi-machine fit reproduced well the shape of the corresponding theoretical curve of $S/XB^{W}_{WI\ 400.9nm}$ deduced from the ADAS data base. The absolute values are are also in a fair agreement with the theoretical ADAS values, but systematically about 50% above the experimental ones. The most likely reason for the discrepancy are not the electron impact excitation rate coeffi-

cients used in ADAS, but the ionisation rate coefficients used for W. Studies outside of this contribution, but from the same experiment with focus on the penetration depth and the velocity of effectively injected W atoms revealed a discrepancy in the experimentally determined ionisation rates when compared with Lotz, ADAS, and GKU calculations [17]. More studies are required to resolve the issue with the ionisation rate coefficients used in ADAS and additional experiments at linear plasma device PSI-2 are currently ongoing.

In this paper also S/XB^{W}_{WI}-values for a number of additional lines were deduced in the spectral range of the overview spectrometer span $(370 - 720nm)$ and the three most prominent lines, namely $429.5nm$, $488.7nm$, and $522.5nm$ have been compared with ADAS calculations. The line shapes of these lines were successfully modelled to ensure that the right transition was identified and no blending is present. The effective $S/XB^{W}_{WI\ 429.5nm}$ and $S/XB^{W}_{WI=\ 522.5nm}$ as function of the electron temperature are in good agreement in shape and magnitude, whereas the $S/XB^{W}_{WI\ 488.7nm}$ is an order away in absolute magnitude. Note that multi-machine fits for these lines were not possible as the data at the low electron temperature range is missing. In this paper also for the first time a $S/XB^{W^+}_{WII\ 434.8nm}$-value for the high electron temperature range was provided, but no ADAS or other experimental data for comparison exists.

It shall be stressed, that the current revisited analysis of the effective S/XB-values of WI are still providing the same W erosion yields as in the earlier studies [6] as the analysis of impurities, tungsten, and deuterium is done within the same spectroscopic system, thus the relative values, the corresponding yields, remain the same. Therefore, the interpretation, that in the case of TEXTOR and W limiters, the sputtering is caused by a mixture of C and O ions is still valid [6, 17] and in agreement with other observations at JET and ASDEX-Upgrade indicated before [3].

Acknowledgments

This work has been carried out within the framework of the EUROfusion Consortium and has received funding from the Euratom research and training programme 2014-2018 under grant agreement No 633053. The views and opinions expressed herein do not necessarily reflect those of the European Commission. This work was done under WP PFC. The authors thank M. O'Mullane for the provision of ADAS calculations for the analysed WI transitions.

References

[1] T. Hirai et al., J. Nucl. Mater. **463** (2015) 1248

[2] R. Neu et al., J. Nucl. Mater. **438** (2013) S34

[3] S. Brezinsek et al., J. Nucl. Mater. **463** (2015) 11

[4] J. W. Coenen et al., Nucl. Fus. **55** (2015) 023010

[5] T. Puetterich et al., Nucl. Fus. **50** (2011) 025012

[6] S. Brezinsek et al., Phys. Scripta **T145** (2011) 014016

[7] R. Dux et al., J. Nucl. Mater. **390-391** (2009) 858

[8] G. van Rooij et al., J. Nucl. Mater. **438** (2013) S42

[9] N. den Harder et al., Nucl. Fus. **55** (2016) 026014

[10] L. Vainshtein et al., Plasma Phys. Control. Fusion **49** (2007) 1833

[11] A. Pospieszczyk et al., J. Phys. B. At. Mol. Opt. Phys. **43** (2010) 144017

[12] http://www.adas.ac.uk/

[13] D. Nishijima et al., Phys. of Plasmas **18** (2011) 019901

[14] A. Geier et al., Plasma Phys. Control. Fusion **44** (2002) 2091

[15] J. Steinbrink et al., ECA (Proc. of the 24th EPS, Berchtesgaden), Vol21A Part IV (1997) 1809

[16] S. Brezinsek et al., Plasma Phys. Control. Fusion **47** (2005) 615

[17] M. Laengner,*phd Thesis University Düsseldorf* (2017), ISSN 0944-2942, Reports of the Forschungszentrum Jülich, Juel-4499, Germany

[18] E. Lassner and W.-D. Schubert, *Tungsten - Properties, Chemistry, Technology of the Element, Alloys, and Chemical Compounds*, ISBN 0-306-45053-4, Springer, Germany

[19] M. Laengner et al., J. Nucl. Mater. **438** (2013) S865

[20] D. Kondratjew et al., J. Nucl. Mater. **438** (2013) S351

[21] U. Kruezi,*phd Thesis University Düsseldorf* (2007), ISBN 978-3-89336-476-3, Schriften des Forschungszentrums Jülich, **62**, Germany

[22] O. Schmitz et al., Plasma Phys. Control. Fusion **50** (2008) 115004

[23] M. Lehnen et al., J. Nucl. Mater.**290-293** (2001) 663

[24] A. Pospiezczyk et al., *High Temperature Plasma Diagnostics*, ISBN 978-3-540-23038-0, Springer Series in Chemical Physics, **Vol78**, Germany

Figure captions:

Fig. 1: a) Experimental set-up with gas inlet location and observation chords of different spectroscopic diagnostics used for the analysis of W emission in the TEXTOR edge plasma. b) 2D emission pattern of WI recorded with an intensified camera equipped with an narrowband interference filter at $\lambda = 400.9nm$. c) Temporal evolution of WI emission at $\lambda = 400.9nm$ during pulsed WF_6 injection into a series of identical plasma discharges (**expA**), but with variation of T_{inlet} by the actively heatable gas inlet system. At higher inlet temperatures ($T_{inlet} > 723K$), WF_6 decomposes in the inlet tube and locally deposits W before entering the plasma causing a reduction in WI emission due to a lower effective W influx.

Fig. 2: Effective inverse photon efficiency for WI at $\lambda = 400.9nm$, or more precise $S/XB^{WF_6 \rightarrow W}_{WI\ 400.9nm}$, as function of (a) edge electron density and (b) edge electron temperature recorded with the Spectrelle system. Values are taken pairwise at the maximum of emission of WI in (**expB**) a series with varying plasma conditions by global deuterium fuelling and constant gas inlet position and (**expD**) a series of constant plasma conditions and varying radial position of the gas inlet in the scrape-off layer. The rate of injected WF_6 into the flat-top phase of the plasma was kept constant in all discharges.

Fig. 3:a) Effective S/XB-values for four different WI transitions as function of the edge electron temperature. All values were taken simultaneously during the WF_6 injection. The comparison with ADAS calculations of S/XB-values as function of T_e is given for a span of n_e covering typical fusion plasma edge conditions. b) Line shape modelling of the analysed WI lines at $\lambda = 400.9nm$, $\lambda = 429.5nm$, $\lambda = 488.7nm$, and $\lambda = 522.5nm$ recorded during

WF_6 injection in TEXTOR at $B_t = 2.25T$.

Fig. 4:.a) Effective inverse photon efficiency for WII at $\lambda = 434.8nm$ as function of the edge electron temperature recorded with the Spectrelle system. b) Line shape modelling of the corresponding WII transition during WF_6 injection in TEXTOR at $B_t = 2.25T$.

Fig. 5:. S/XB-value for WI at $\lambda = 400.9nm$ as function of the electron temperature deduced from different experiments and methods including weight loss [13] in PISCES-B, $W(CO)_6$ evaporation in ASDEX-Upgrade [14] and PSI [15] at the low T_e-range as well as WF_6 injection in TEXTOR at the high T_e-range analysed by two spectroscopic systems with the corresponding uncertainties indicated. The experimental data has been fitted by a least-square fit routine providing a multi-machine scaling valid in the range of approximately $T_e \simeq 2eV$ and $T_e \simeq 85eV$. For comparison are S/XB-values from ADAS for the same optical transition as function of T_e shown.

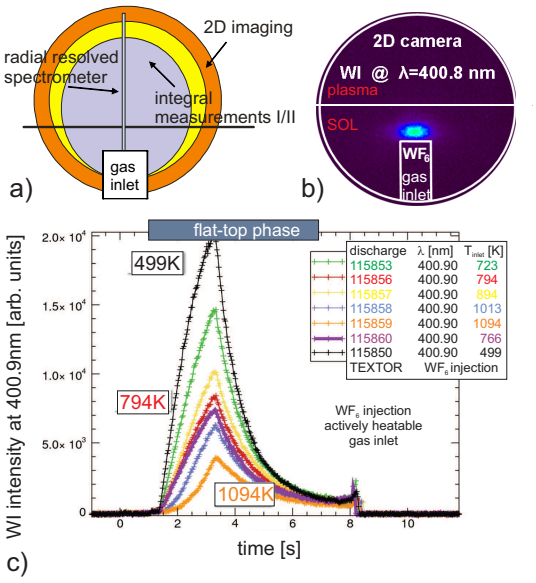

Figure 1:

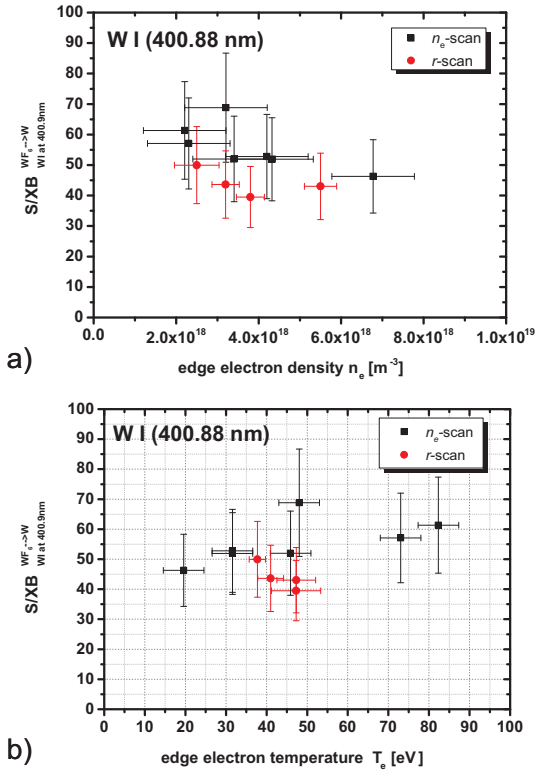

Figure 2:

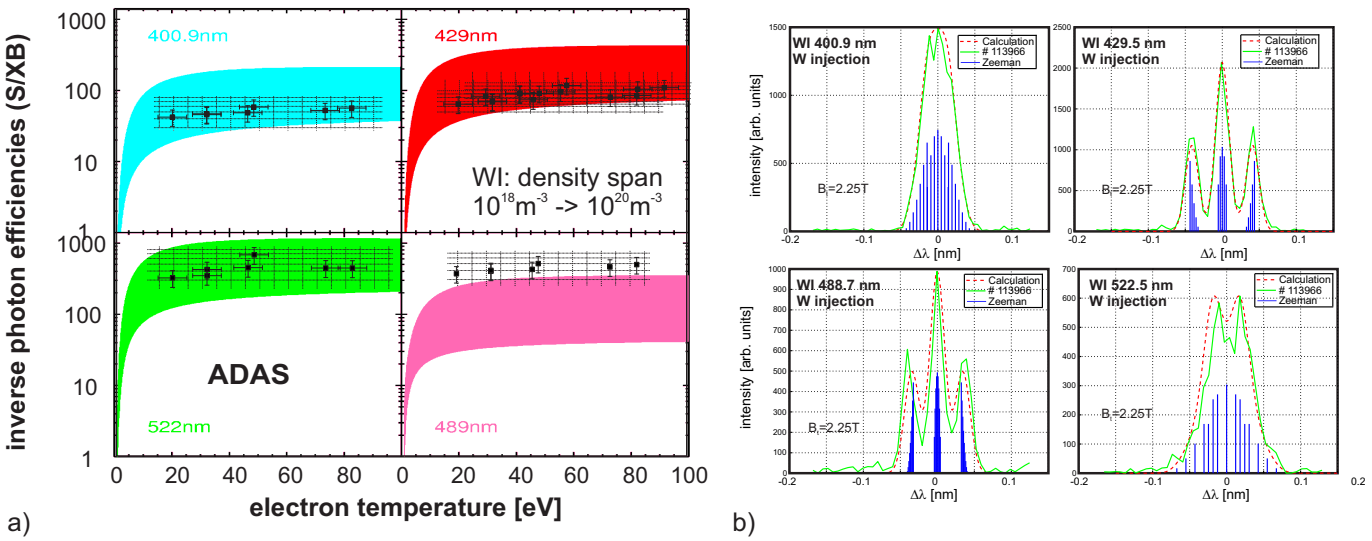

Figure 3:

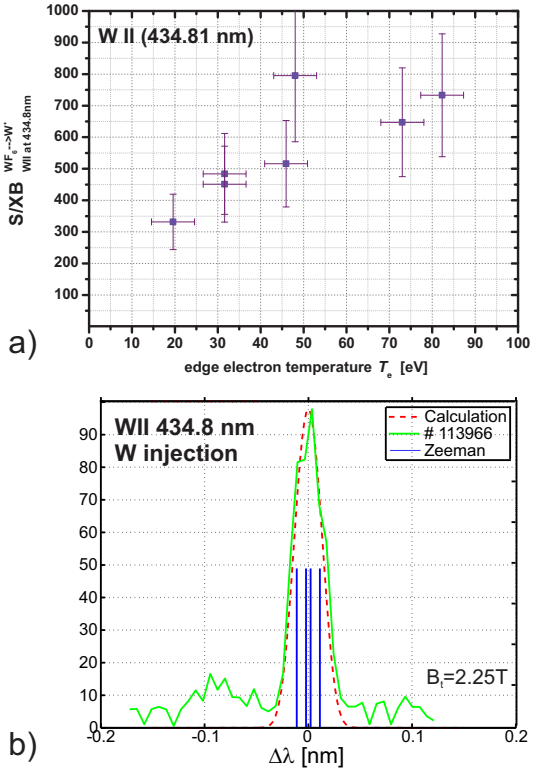

Figure 4:

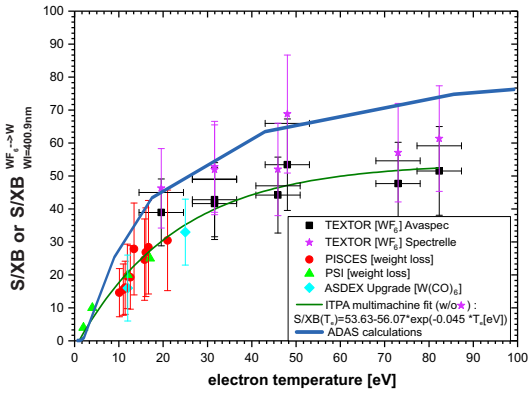

Figure 5: